NAL PROPOSAL No. 326

Scientific Spokesman:

P. A. Piroué
Department of Physics
Joseph Henry Laboratories
Princeton University
Princeton, New Jersey 08540

FTS/Off-net: 8 (609) 599-3511
452-3000

A PROPOSAL TO MEASURE MUON PAIRS PRODUCED AT HIGH TRANSVERSE MOMENTUM BY PIONS

J. W. Cronin, H. J. Frisch, and M. J. Shochet
The Enrico Fermi Institute, University of Chicago
Chicago, Illinois 60637

and

J. P. Boymond, P. A. Piroué, and R. L. Summer
Department of Physics, Joseph Henry Laboratories
Princeton University, Princeton, New Jersey 08540

June 1974

PROPOSAL #326

Formerly

ADDENDUM TO NAL PROPOSAL 258

J. P. Boymond, P. A. Piroue*, and R. L. Sumner
Department of Physics, Joseph Henry Laboratories
Princeton University, Princeton, New Jersey 08540

and

J. W. Cronin, H. J. Frisch, and M. J. Shochet
The Enrico Fermi Institute
University of Chicago, Chicago, Illinois 60637

May 29, 1974

*Correspondent

ADDENDUM TO NAL PROPOSAL 258

J. P. Boymond, P. A. Piroue*, and R. L. Sumner
Department of Physics, Joseph Henry Laboratories
Princeton University, Princeton, New Jersey 08540

and

J. W. Cronin, H. J. Frisch, and M. J. Shochet
The Enrico Fermi Institute
University of Chicago, Chicago, Illinois 60637

May 29, 1974

*Correspondent

We propose the construction of a muon detector on the other side of the incident π beam from the focusing spectrometer. Such a muon detector would permit a very sensitive search for the process $\pi^- + \text{nucleon} \rightarrow \mu^+\mu^- + X$ in addition to the proposed measurement of hadron and muon production at high $P_\perp$.

The rate for the reaction $\pi^- p \rightarrow \mu^+\mu^- + X$ is predicted [1,2,3] to be enhanced over that in proton-proton collisions by the parton model. This is due to the fact that a π^- has a "fast" anti-quark component, thereby facilitating the quark-antiquark annihilation into a high mass virtual photon, which then decays to a muon pair. Parton model predictions[2] for the invariant cross sections for single muons from proton-proton and π^- proton collisions are shown in Figure 1; one sees that at 300 GeV single muon production from pions is at least 10 times more copious than that from protons at $P_\perp = 3$ GeV/c.

The spectrum of single directly produced muons has already been measured in proton-proton collisions[4]; attachment A to this addendum is a report on our results from such a measurement performed in NAL Experiment 100. The results of this measurement are shown in Figure 3 of the attachment. The measured muon spectrum has the same shape as the pion spectrum, but is suppressed by a factor of $\sim 10^{-4}$. Figure 3 also shows the parton model[2] prediction for the single muon spectrum: one sees that even down to very small cross sections it is completely buried beneath the measured spectrum. Consequently, tests of the parton model predictions in p-p collisions must rely on the detection of muon pairs.

Figure 1 shows the situation for pion induced single muons -- one sees that if the production of muons by pions is the same as that measured with protons, it will be equal to the parton model predictions at $P_\perp \approx 4$ GeV/c, and at an invariant cross section $Ed\sigma/d^3p = 3 \times 10^{-37}$ cm^2 GeV^{-2}. This cross section is measurable with a π^- beam of 10^{10}/pulse at NAL. If the directly produced single muons measured at NAL are produced in low invariant mass pairs, such as the ρ, ω,ϕ, etc., then the requirement of detecting the second muon should provide the required discrimination to separate these events from those coming from high invariant mass pairs.

A possible layout for the spectrometer and the muon arm is shown in Figure 2. The central angle would be 100 mr, 90° in the c.m. for a 200 GeV/c incident beam. The muon arm subtends between 35 and 160 mr in the lab, and has an acceptance of 50 mr in azimuth. Three banks of scintillator hodoscopes separated by absorber determine the muon direction and identification.

Because of the requirement of transverse momentum balance, if the muon pair is assumed to have zero initial transverse momentum, the determination of the angle of the second muon is enough to determine its momentum. The invariant mass of the pair is already determined by the transverse momentum.

Figure 3 shows the rates for single muons and muon pairs in events/shift vs. $P_\perp$ measured in the spectrometer arm, as computed from the parton model calculation of G. Farrar[2]. At a $P_\perp$ of 3 GeV (invariant mass = 6 GeV/c^2), and with a 200 GeV beam of 10^{10} pions/pulse, one detects 8 events/shift. The one event/shift level is reached at a $P_\perp$ of 5 GeV/c.

In addition to adding the muon arm, we also have made some simple modifications to the NAL 100 spectrometer design that have increased its

solid angle by a factor of 2 to 32 μster and its momentum bite to ± 10%. This results in an increase of a factor of 4 in rate over the proposal values. The modifications consist of shortening the spectrometer so that the maximum measurable $P_\perp$ is 10 GeV/c, and replacing the main ring quadrupoles and bend magnets currently in use with 4Q 120 beam transport quadrupoles and 6-3-120 bend magnets, respectively. The new magnets have the added advantage that they run at much more reasonable currents than the present ones.

REFERENCES

1. R. P. Feynman, Photon Hadron Interactions, Benjamin, p. 163 (1972).
2. G. Farrar, CALTECH preprint CALT-68-422.
3. M. Einhorn and R. Savit, NAL preprint, NAL PUB-74/35-THY.
4. J. P. Boymond et al., see attached preprint (to be published). Also similar results have been presented at the Washington meeting by NAL experiments 70 and 184.

FIGURE CAPTIONS

Figure 1. Predictions of Farrar[2] for single muon production in pp (dotted curves) and π^- p collisions. The triangles represent 10^{-4} times the single pion production in proton-W collisions - this is a likely background of prompt muons.

Figure 2. A possible layout for the charged particle spectrometer and the muon arm.

Figure 3. Rates in events/shift for single muons and muon pairs for the apparatus described, as predicted by the model of Farrar.[2]

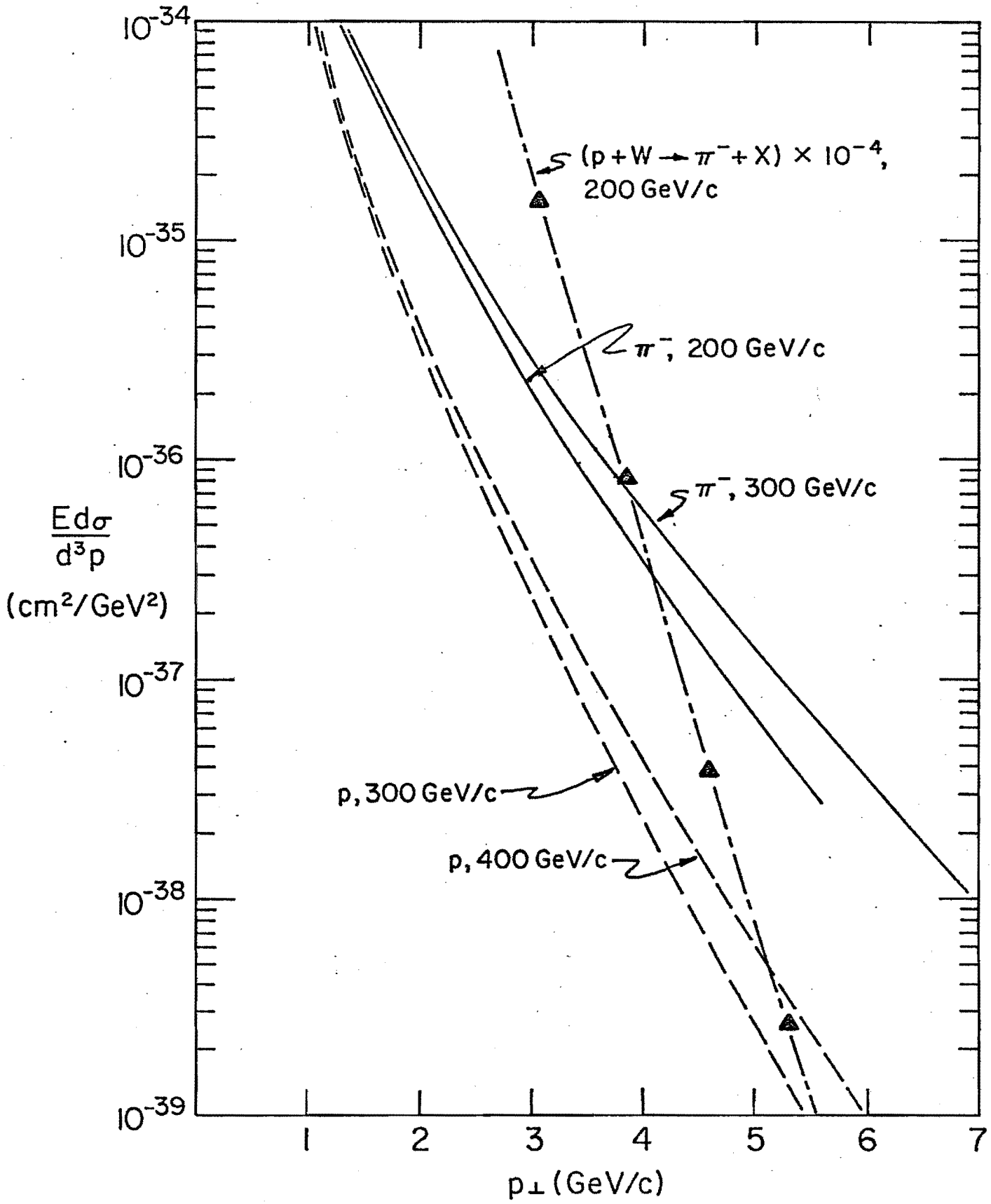
10^{-34}
10^{-35}
10^{-36}
10^{-37}
10^{-38}
10^{-39}
$\frac{E d\sigma}{d^3p}$
(cm^2/GeV^2)
$(p + W \rightarrow \pi^- + X) \times 10^{-4}$, 200 GeV/c
π^-, 200 GeV/c
π^-, 300 GeV/c
p, 300 GeV/c
p, 400 GeV/c
1
2
3
4
5
6
7
$p_\perp$ (GeV/c)

Figure 1

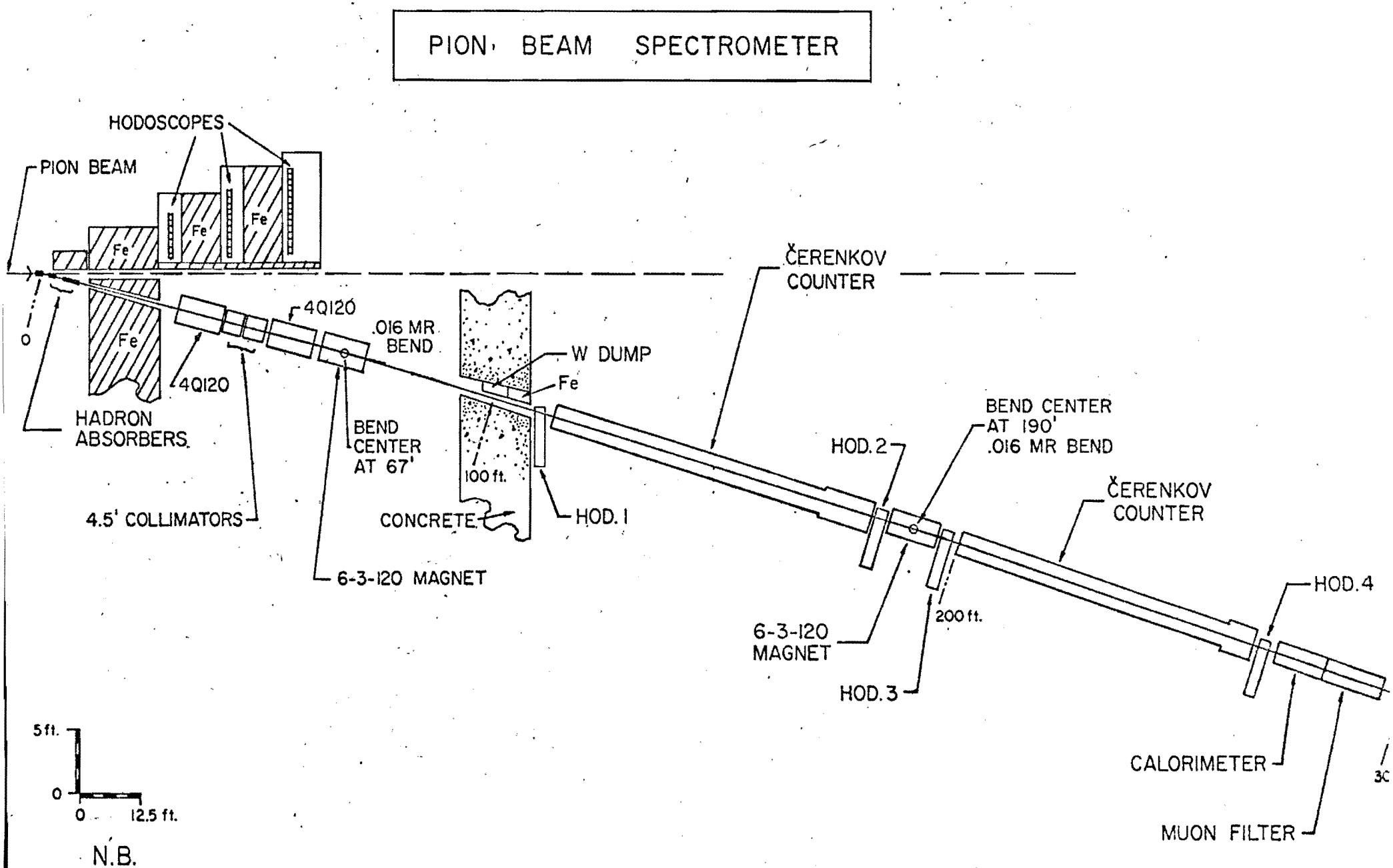
PION BEAM SPECTROMETER
HODOSCOPES
PION BEAM
Fe
Fe
Fe
Fe
0
HADRON ABSORBERS
4Q120
4Q120
.016 MR BEND
BEND CENTER AT 67'
4.5' COLLIMATORS
6-3-120 MAGNET
W DUMP
Fe
100 ft.
CONCRETE
HOD. 1
ČERENKOV COUNTER
HOD. 2
BEND CENTER AT 190' .016 MR BEND
ČERENKOV COUNTER
6-3-120 MAGNET
200 ft.
HOD. 3
HOD. 4
CALORIMETER
MUON FILTER
5 ft.
0
0
12.5 ft.
N.B.

Figure 2

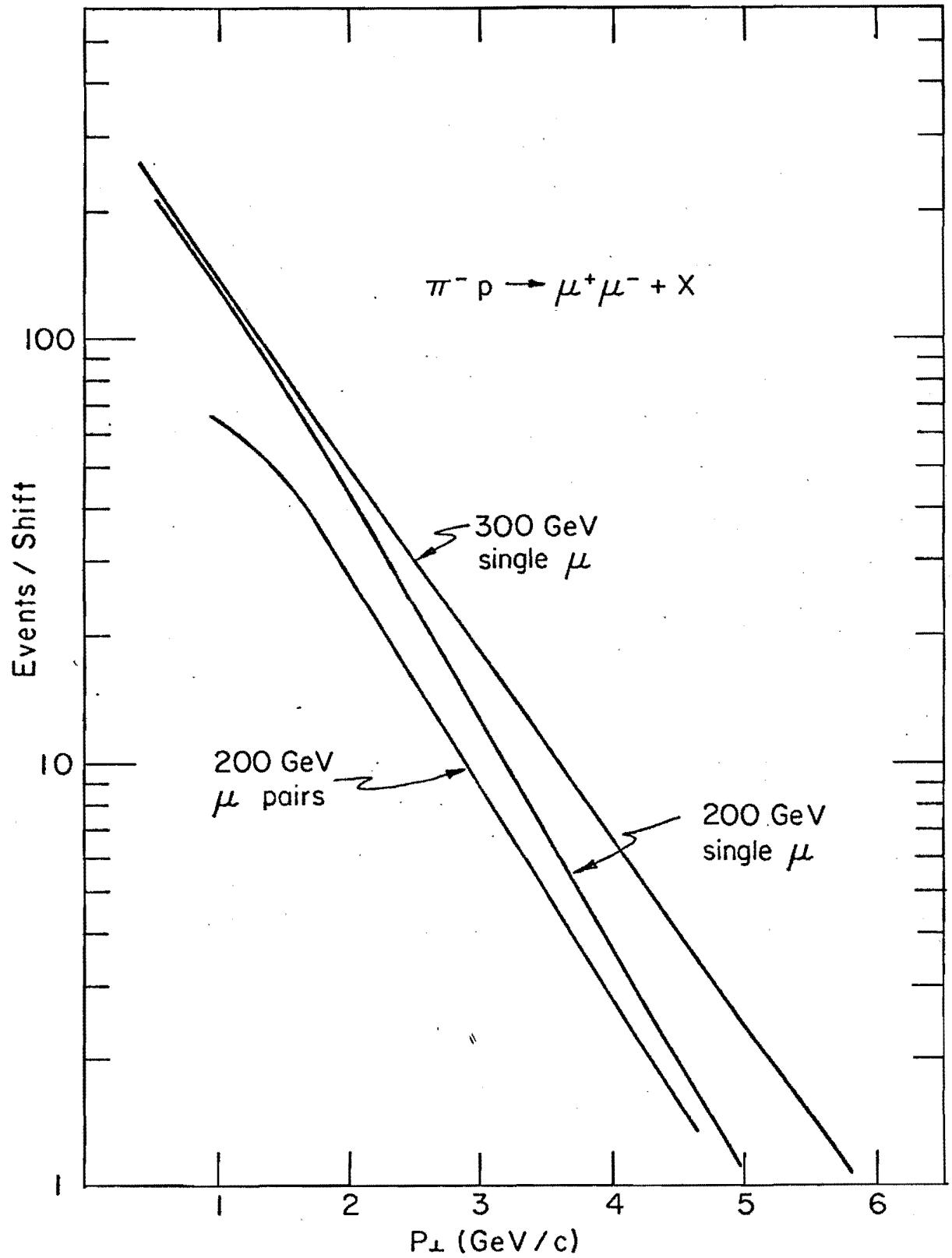
$\pi^- p \rightarrow \mu^+\mu^- + X$
100
10
1
Events / Shift
300 GeV
single μ
200 GeV
μ pairs
200 GeV
single μ
1
2
3
4
5
6
$P_\perp$ (GeV / c)

Figure 3

EFI-74-24

Observation of Large Transverse Momentum Muons Directly Produced by 300 GeV Protons*

J. P. Boymond, R. Mermod,† P. A. Piroué, and R. L. Sumner
Department of Physics, Joseph Henry Laboratories
Princeton University, Princeton, New Jersey 08540
and
J. W. Cronin, H. J. Frisch, and M. J. Shochet
The Enrico Fermi Institute
University of Chicago, Chicago, Illinois 60637

ABSTRACT

We have observed muons produced directly in Cu and W targets by 300 GeV incident protons. We find a yield of muons which is approximately a constant fraction (0.8×10^{-4}) of the pion yield for both positive and negative charge and for transverse momenta between 1.5 and 5.4 GeV/c.

In this letter we report on the observation of muons produced directly in nuclear targets by 300 GeV incident protons. Study of muon production at high transverse momentum was originally motivated by the search for the intermediate vector boson. Early experiments were carried out at the Argonne Z.G.S.[1] and the Brookhaven A.G.S.[2] with negative results. More recently, several experiments have shown evidence either for the direct production of single muons,[3,4] or muon pairs[5] in nucleon-nucleon collisions. Extensive theoretical work[6,7] suggests

that collisions of point-like constituents of the nucleon would result in the direct production of muons.

In this experiment, performed at the National Accelerator Laboratory (NAL), we have used an apparatus described in a previous publication.[8] It consists of a single arm focusing spectrometer equipped with two Cerenkov counters and a calorimeter to identify hadrons, and a 15-ft.-long steel filter sampled each 2.5 ft. with dE/dx counters to identify muons. The spectrometer viewed secondaries produced in a heavy target at an angle of 77 mrad relative to the incident 300-GeV proton beam. This angle corresponds to $\sim 90°$ in the nucleon-nucleon c.m. Direct muons from the target were separated from muons coming from π and K decays in flight with the aid of two absorbers which could be inserted into the spectrometer close to the target. The first absorber was a 23-in.-long W block with its upstream face 9.5 in. from the center of the target. The second absorber was a 42-in.-long Fe block with its upstream face 42 in. from the target. We used a 2-in.-long W target, primarily in runs with negative muons, and a 3-in.-long Cu target primarily in runs with positive muons.

Data were taken under three conditions: 1) no absorber, 2) W absorber inserted only, and 3) Fe absorber inserted only. Runs were made at 10 GeV/c intervals between 20 GeV/c and 70 GeV/c corresponding to transverse momenta ($P_\perp$) from 1.5 to 5.4 GeV/c. At 20 and 30 GeV/c, data were also taken with both absorbers in the beam as a consistency check. To verify that the muons were associated with the target, we also took data with the target removed for the three principal conditions at 20, 30 and 40 GeV/c.

For each absorber condition we measured the ratio of muons detected at the end of our apparatus to pions of the same charge detected by the apparatus

when the absorber was absent. Two counter telescopes which looked at the target at 90° laboratory angle permitted normalization of different runs. The yield of pions with no absorber was corrected for nuclear absorption in the remainder of the apparatus and for decay in flight.

The hadrons were attenuated by factors of $\sim$ 200 and $\sim$ 270 with the W and Fe absorbers respectively. These rather small attenuations resulted in a significant hadron penetration. These hadrons were identified by the combination of the Cerenkov counters and the hadron calorimeter. Those decaying appeared as muons. Thus the observed muons with absorber in place consisted of three components: 1) muons produced directly in the target, 2) muons produced by hadrons decaying upstream of the absorber, and 3) decay muons from hadrons which penetrated the absorber.

For process (3) the ratio of muons to pions[9] was directly measured at each momentum and polarity in runs without the absorbers; the corresponding muon yield in the absorber runs is calculated from the observed penetrating pions. The remaining muon yield coming from processes (1) and (2) is then corrected for the loss due to the absorber insertion (e.g. multiple scattering). Finally, the direct muon yield is obtained by linear extrapolation to zero decay path.

In Table I we present the reduction of the raw data from a typical run at 40 GeV/c. The absorber loss factors, calculated by Monte Carlo techniques, are presented in Table II. These factors account for the multiple scattering loss, as well as the increased yield due to acceptance of smaller $P_\perp$ when the absorber is in place. The dependence of yield on $P_\perp$ was taken from our previous measurements of hadron production.[8] We thus assume that the direct muon component has a similar dependence on $P_\perp$, an assumption that can be checked à postiori.

Figure 1 shows the corrected results of a typical run along with the predicted slope. The points are plotted at a distance $(d + \lambda)$ where d is the distance between the target and the upstream end of the absorber, and λ is the measured interaction length in the absorber.

The predicted slope can be obtained from the rate of hadron decay between the target and the absorber. It was calculated by numerical integration as a function of momentum. The yield of decay muons between the target and absorber depends on both K and π decays. Kaons are twice as effective as pions in producing detected muons. Thus the slope is sensitive to the K/π ratio at the target. Figure 2 shows for both charges the predicted and observed slopes plotted against the inverse of the muon momentum.

The agreement between calculated and observed slopes is a significant verification of the corrections which are quite different in nature for the two absorbers. The W absorber is more sensitive to the broadening of the acceptance because of its proximity to the target, but is less sensitive to multiple scattering for the same reason. The inverse is true for the Fe absorber.

Table III gives the ratio of direct muons to pions at the target for all conditions. The most striking aspect of these results is the constancy of the ratio μ/π. The constancy for different target materials is particularly interesting. In a separate experiment, to be reported in a subsequent publication, we have found the yield of pions per interacting proton at 3 GeV/c $P_\perp$ to be 3.5 times larger from a W target than a Be target. This effect is believed to be due to secondary scattering in the nucleus. Since the direct muons follow the same pattern, a strongly interacting, short lifetime source is suggested for the muons.

One such source can be the known vector mesons. For example, if ρ and ϕ were each produced with the same cross section as π, we would expect a ratio $(\mu/\pi) \times 10^4$ of 0.68, 0.46, and 0.33 at $P_\perp$ of 1.5, 3.0, and 4.5 GeV/c respectively.

In Figure 3 we plot the invariant cross section per nucleon for inclusive muon production. Also plotted is the inclusive pion cross section $\times 10^{-4}$ and the inclusive muon cross section expected from a model based on parton-antiparton annihilation.[10] It is clear that the yield of muons is everywhere in excess of the parton model prediction.

We wish to thank the staff of the Proton Section of NAL for their magnificent support of this experiment. We also wish to thank V. L. Fitch, S. B. Treiman, E. A. Paschos, and G. R. Farrar for valuable discussions. Finally, one of us (R.M.) wishes to thank NAL for its hospitality and support.

REFERENCES

*Work supported by the National Science Foundation and the U. S. Atomic Energy Commission.

†On leave at NAL from the University of Geneva.

1. R. C. Lamb et al., Phys. Rev. Letters 15, 800 (1965).
2. R. Burns et al., Phys. Rev. Letters 15, 830 (1965).
3. P. J. Wanderer et al., Phys. Rev. Letters 23, 729 (1969).
4. Bondarenko et al., (Paper 927), Proceedings of the XVI International Conference on High Energy Physics, Vol. 2, p. 329, (1972), edited by J. D. Jackson and A. Roberts.
5. J. Christenson et al., Phys. Rev. Letters 25, 1523 (1970).
6. S. D. Drell and T. M. Yan, Phys. Rev. Letters 25, 316 (1970).
7. J. D. Bjorken, Proceedings of II International Conference on Elementary Particles, Aix-en-Provence (1973), Journal de Physique, 34, C1-385, (1973).
8. J. W. Cronin et al., Phys, Rev. Letters 31, 1426 (1973).
9. For convenience we normalize to pions; the pions serve as a measure of all hadrons.
10. G. R. Farrar, California Institute of Technology preprint, CALT - 68 - 422, (1974); also private communication.

FIGURE CAPTIONS

Figure 1. Plot of data reduced in Table I. The dashed curve shows the linear extrapolation to the target. The solid line is the calculated slope.

Figure 2. Plot of observed slope and calculated slope vs. reciprocal of the muon momentum. The points are the experimentally measured slopes; the solid line is the calculated slope.

Figure 3. Plot of the invariant cross section for direct muon production vs. $P_{\perp}$. Also shown is the pion cross section x 10^{-4} and the cross section predicted by a parton model

TABLE CAPTIONS

Table I. Reduction of raw data to direct muon yield at the target. Processes (1), (2), and (3) are referred to in the text. Tungsten and Iron refer to the particular absorber used.

Table II. Calculated absorber loss factors.

Table III. Ratio of directly produced muons to pions in the proton-nucleus collision. The observed pions emerging from the 0.4-interaction-length target are multiplied by a factor 1.25 to account for absorption in the target itself.

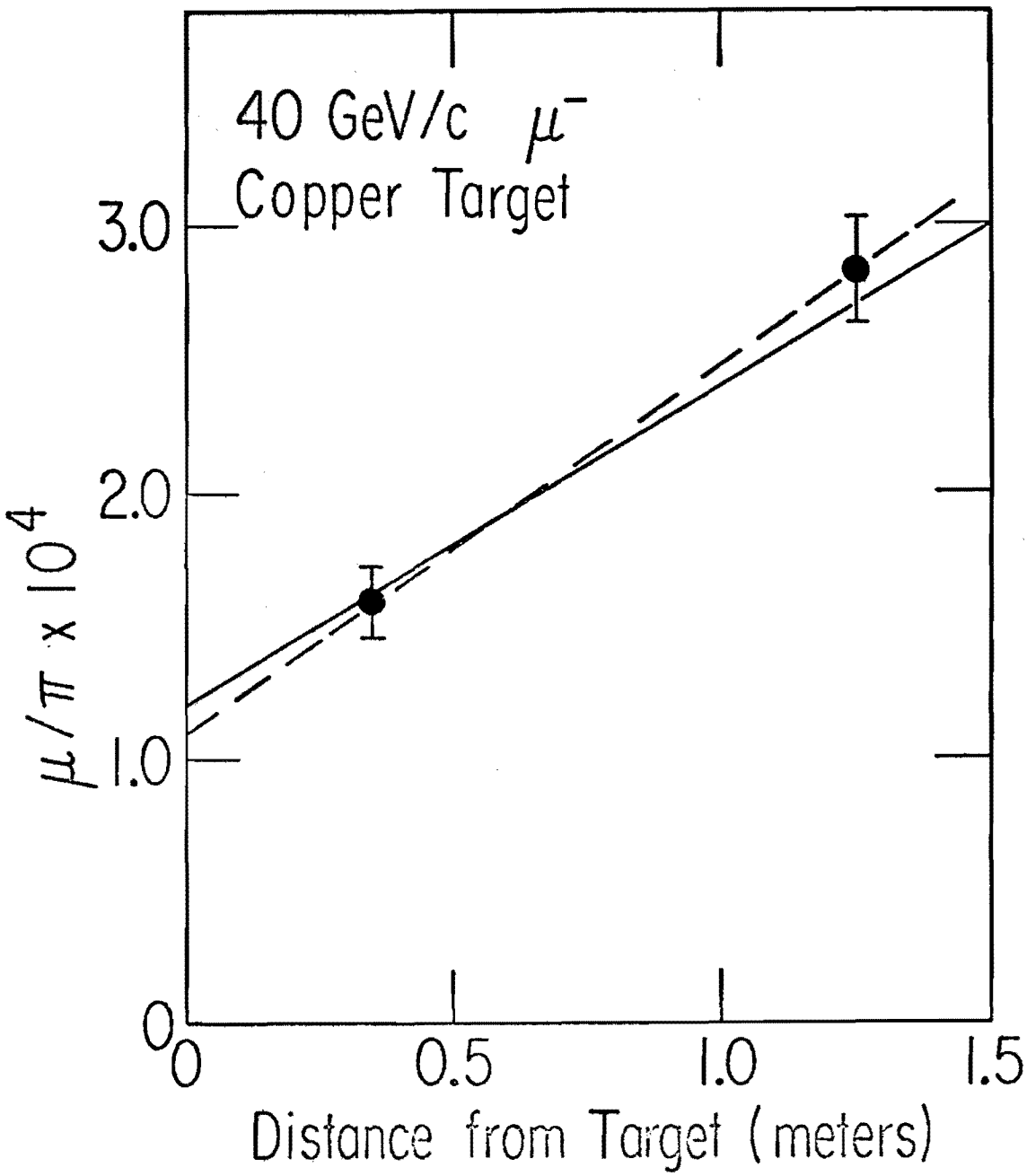
40 GeV/c μ^-
Copper Target
3.0
2.0
1.0
0
$\mu/\pi \times 10^4$
0
0.5
1.0
1.5
Distance from Target (meters)

Figure 1

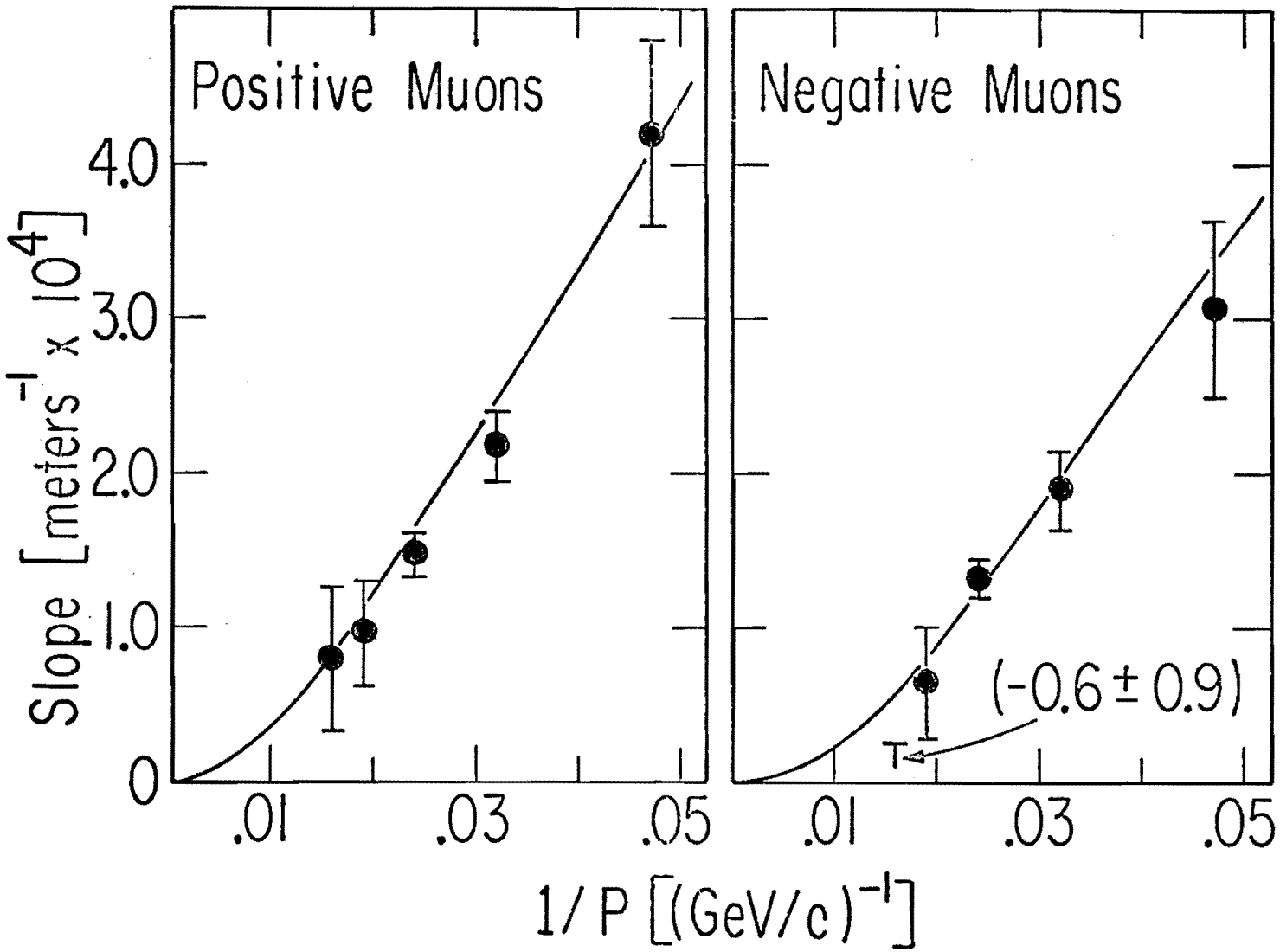
Positive Muons
Negative Muons
Slope [meters^{-1} x 10^4]
4.0
3.0
2.0
1.0
0
.01
.03
.05
(-0.6 ± 0.9)
1/ P [(GeV/c)$^{-1}$]

Figure 2

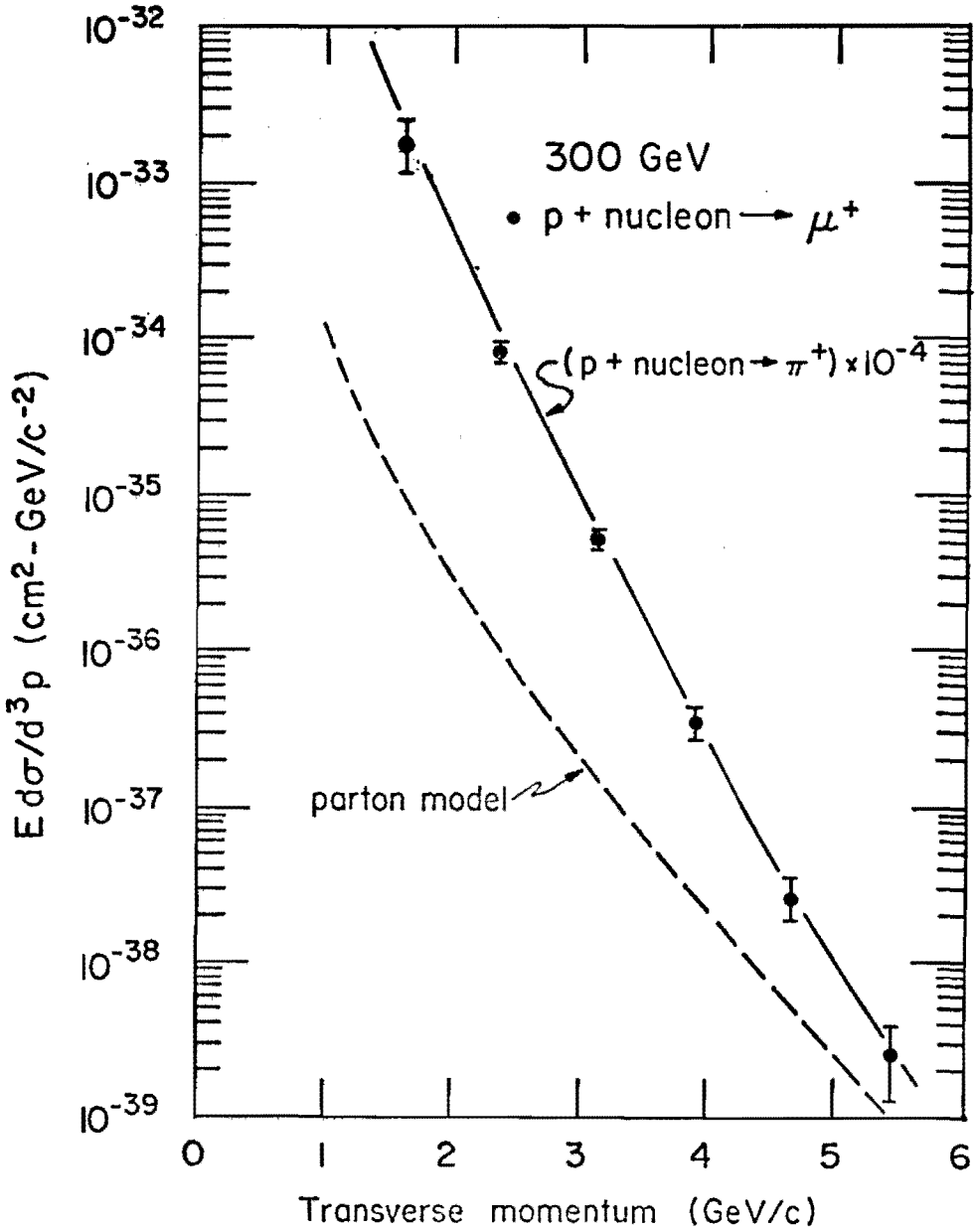
300 GeV
• p + nucleon → μ+
(p + nucleon → π+) × 10-4
parton model
E dσ/d3p (cm2 - GeV/c-2)
Transverse momentum (GeV/c)
10-32
10-33
10-34
10-35
10-36
10-37
10-38
10-39
0
1
2
3
4
5
6

Figure 3

	Tungsten	Iron
Observed muons	795±28	623±25
Observed pions	13580	4985
Ratio μ/π without absorber	$(2.03\pm0.10) \times 10^{-2}$	
Muons from hadron penetration of absorber (process (3))	276±13	101±5
Muons from processes (1) and (2)	519±31	522±26
Absorber loss factor	0.71±0.04	0.40±0.02
Corrected muons from processes (1) and (2)	731±60	1305±92
Pions at target	4.60×10^{6}	4.62×10^{6}
Muons/Pions at target	$(1.59\pm0.13) \times 10^{-4}$	$(2.83\pm.20) \times 10^{-4}$
Effective distance to target (meters)	0.35	1.25
Extrapolated μ/π at target	$(1.10\pm0.15) \times 10^{-4}$	

Table I

Momentum (GeV/c)	Tungsten	Iron
20	0.42±0.03	0.182±0.015
30	0.56±0.03	0.300±0.015
40	0.71±0.04	0.40±0.02
50	0.81±0.05	0.47±0.02
60	0.87±0.04	0.54±0.02
70	1.02±0.04	0.62±0.03

Table II

$P_\perp$ (GeV/c)	$\mu/\pi \times 10^4$ (Target) Positive	Negative
1.62	.66±.25 (Cu)	.86±.20 (W)
2.38	.72±.11 (Cu)	.67±.12 (W)
3.15	.88±.18 (Be)	- - -
3.15	.94±.16 (Cu)	.88±.12 (Cu)
3.15	.60±.15 (W)	.74±.16 (W)
3.91	.98±.23 (Cu)	.88±.26 (W)
4.67	.87±.30 (Cu)	1.02±.34 (W)
5.44	.94±.47 (Cu)	1.20±.46 (W)

Table III

ADDENDUM TO NAL PROPOSAL 326

J. W. Cronin, H. J. Frisch, and M. J. Shochet
The Enrico Fermi Institute
University of Chicago, Chicago, Illinois 60637

and

J. P. Boymond, P. A. Piroué, and R. L. Sumner
Department of Physics, Joseph Henry Laboratories
Princeton University, Princeton, New Jersey 08540

August 12, 1974

ADDENDUM TO PROPOSAL 326

I. Introduction

We have made further calculations on the design of a second spectrometer arm to detect muons in coincidence with the wide angle precision spectrometer described in NAL Proposal 258. The design described in this addendum provides a simple, very large solid angle device capable of giving a mass resolution of $\frac{\Delta m}{m} \lesssim 10\%$.

II. Motivation

The muon arm would be used in coincidence with the precision spectrometer in a mode whereby a trigger in the spectrometer would latch the counters of the muon arm. As the precision spectrometer can be set to measure either hadrons or directly produced muons, one can search for both dimuon events and hadron-muon coincidences.

The dimuon mass spectrum has been measured in proton-proton collisions at BNL[1]. At present there are experiments set up both at BNL, NAL, and the ISR to detect lepton pairs in p-p collisions, and there are further such proposals to NAL. However, neither the single lepton production nor the pair spectrum has been measured for πp collisions.

Parton model calculations[2,3] predict that the production of large invariant mass muon pairs is enhanced in $\pi^- p$ collisions by more than an order of magnitude over that in p-p collisions. This enhancement reflects the component of "fast" anti-quarks inherent in a pion beam. Specifically, the source of muon pairs in the parton model is the annihilation of a quark and an anti-quark into a virtual photon, which then decays into a lepton pair[2,3]. The energy of the photon is given by

$$E_\gamma = \sqrt{x_1 x_2 s}$$

where $\sqrt{s}$ is the c. m. energy of the primary collision, and x_1 and x_2 are the fractions of the incident particles momenta carried by the quark and anti-quark, respectively. In the proton the distribution in x of anti-quarks is cut off sharply approximately as $(1 - x)^7$, thus limiting the values of E_γ produced. In the pion, however, as the state with the fewest constituents is the quark-anti-quark state, the distribution for the anti-quark is like that for the quark, and is thus less steep than $(1 - x)^7$. Consequently, both x_1 and x_2 can be appreciably different from zero, and the production of high mass photons in πp collisions is predicted to be enhanced over that in pp collisions.

Recent surprising results on e^+e^- collisions from SPEAR[4], and on deep inelastic scattering from NAL[5] have cast doubt on the parton model. As both the dilepton production in hadronic collisions and the e^+e^- annihilation into hadrons procede via a heavy virtual photon, the

two processes are intimately related[6]. The measurement of dilepton pairs from πp collisions can add another important test of the ideas inherent in the parton model -- in particular, if experimentally the dilepton production is not enhanced over that in pp collisions, one has completely destroyed the fundamental notions of quark-anti-quark annihilation into lepton pairs.

Another use of the muon arm would be as a means of conducting searches for unknown objects and processes by looking for a hadron in the precision spectrometer accompanied (i.e., in coincidence) by a muon in the second arm. With its two long Čerenkov counters, the precision spectrometer has the important capacity of identifying the particle type of large transverse momentum hadrons up to the highest momentum likely to be seen at NAL. One could thus use the combination of the spectrometer and the large solid angle muon arm to look for the coincidence of a specific type of hadron and a muon. A possible example of such a signature might be the production of a pair of charmed particles which decay via the mode $x \rightarrow K\mu\nu$. If, as currently thought, the charmed particles are short-lived ($\sim 10^{-13}$ sec), one would expect to see direct muons in coincidence with kaons at some level.

III. The Dilepton Layout

A plan view of the proposed muon arm and the precision spectrometer is shown in Figure 1. As described in Proposal 258, the precision spectrometer views the target at an angle of $\sim$ 100 mr from the pion beam, corresponding to an angle of 90° in the c.m. at 200 GeV. On the other

side of the beam, the proposed muon arm design would cover the angular range from 40 mr to 160 mr in the lab, corresponding to angles from 45° to 120° in the c. m. The detector would require an enclosure approximately 140' long and 15' wide -- this is comparable to the enclosures presently planned in the location where this detector would be placed.

An enlarged view of the muon arm is shown in Figure 2. The detectors in the muon arm would consist of five 4' x 5' counter hodoscopes, set up in an array such that a muon would penetrate at least two of the hodoscopes. The hodoscope slats would be on the order of 6" wide, i. e., comparable to the multiple scattering induced deviations. The vertical slats give directly the opening angle of the second muon; the horizontal slats do not enter into the invariant mass calculation, but give additional information about the production plane of the pair.

The momentum measurement of the second muon is made with three solid iron magnets, each with an array of 4 multiwire proportional counters (MWPC) with wires only in the horizontal direction; as the magnets bend in the vertical plane,this serves to measure the momentum. The momentum measurement is governed by the multiple scattering in the solid magnet -- for a 10' magnet, one would have a resolution of $\Delta p/_p \simeq$ 11%.

The design relies on having counters spaced in a linear array parallel to the beam line. We have thus chosen a detector geometry which has a minimum range requirement for a muon to penetrate corresponding to a fixed minimum transverse momentum, <u>independent of angle</u>. This the right criterion because the limiting factor in how close one can get to an

intense beam interacting in a target behind a shield wall is given by the flux of muons from decaying pions and kaons produced at the target. As the π and K production spectra are very steep with transverse momentum, most of the muons come from the low transverse momentum hadrons, where the production is not sharply angle dependent. For the design shown in Figure 1, the minimum $p_\perp$ required for a muon to penetrate to the detector is 1.5 GeV, although the lab momentum required ranges from 9.4 GeV at 160 mr to 37.5 GeV at 40 mr.

The azimuthal acceptance also obeys a similar kind of invariance, i. e., it has a constant cutoff in the component of transverse momentum in the vertical direction. For instance, for events with a horizontal component of $p_\perp$ of 3 GeV, the counters in the muon area will accept muons which have up to 1 GeV of $p_\perp$ in the vertical direction, again independent of the production angle.

To keep the length of the detector manageable, we have chosen to use steel rather than dirt as the range shield. A moveable high density (e.g., tungsten) shutter close to the target allows a measurement of the muon background due to hadron decay.

IV Detailed Properties of the Detector

A. Acceptance

The detector accepts particles with angles to the beam in the angular range from 40 mr to 160 mr in the lab, corresponding to a coverage from 45° to 120° in the c.m. for 200 GeV incoming pions. The azimuthal coverage of the counter hodoscopes varies from ± 50 mr at 160 mr to ± 13 mr at 40 mr. The azimuthal coverage of the magnetized iron spectrometer system is half that of the counter system. However one could easily use the field in the return legs to double the coverage of the magnet system.

This angular coverage of the counter system gives a solid angle of 900 mster in the c.m. at 200 GeV; the magnetic spectrometer covers 450 mster. (This is to be compared to the approximately 4 mster of the precision spectrometer).

The minimum detectable $P_{\perp}$ for the second muon is 1.5 GeV. This obviously limits the possible masses of the parent particle to masses greater than 3 GeV, assuming no horizontal transverse momentum for the parent. (Any transverse momentum of the parent particle clearly allows one to detect parents of lower masses with reduced efficiency.) The area of the Peyrou plot covered by the muon arm is shown in Fig. 3.

B. Sensitivity to Muon Pairs

From estimates of the proton and pion structure functions, one can estimate from the parton model the efficiency for detecting the "other" muon from the pair in the muon arm, given that the precision spectrometer has triggered on one muon. Fig. 4 shows the angular distribution $\frac{d\sigma}{d\theta}_{lab}$ for the second muon for various settings in $P_{\perp}$ for the spectrometer, as calculated

by G. Farrar.[3] The integral of these curves between 40 and 160 mr gives the fraction of events in which the other muon is accepted -- this is shown vs. $P_\perp$ in Fig. 5.

The calculated rates for detecting μ pairs vs. $P_\perp$ is shown in Fig. 6, assuming an incident beam of 10^{10} π^-/ pulse at 200 GeV. One can detect pairs with masses up to $\sim$ 10 GeV with this system if the parton model predictions are correct.

C. Accidental Rates

The accidental rates from muons from π and K decay have been calculated assuming:

1) an 18" decay distance (conservative)
2) $E \frac{d\sigma}{dp^3}$ as measured at 300 GeV by NAL 100.
3) $E \frac{d\sigma}{dp^3}$ is independent of angle.

The rates in each counter bank are shown in Table I, assuming 10^{10} interacting π^-/pulse. The total rate in the hodoscope system is $\sim 1.5 \times 10^4$/ pulse. Assuming a time resolution of 20 nsec and an effective spill length of 500 msec, this total rate corresponds to an accidental background of $\sim 6 \times 10^{-4}$; i. e., one can detect at that level processes which occur in coincidence with a particle in the precision spectrometer. For instance, if only 1% of the direct muons detected in the precision spectrometer have an accompanying wide angle muon on the other side, then with a detection efficiency of 60% for the muon arm, the signal/background ratio will be approximately 10:1.

D. Multiple Scattering and Energy Loss

The root-mean-square angles and displacements from multiple scattering of a muon with $P_\perp$ = 3 GeV are shown in Table II. The major effects

of multiple scattering are:

1) to decrease the acceptance from scattering in the vertical plane, and
2) to limit the invariant mass resolution by changing the measured opening angle.

From Table II one can see that the 4' high vertical acceptance of the counter hodoscopes is everywhere appreciably larger than the mean displacement from multiple scattering, so that there is only a very small decrease in acceptance. For the magnet geometry, the problem is more serious, as the displacements start to become comparable to the magnet dimensions. Table II shows the loss due to multiple scattering as a function of angle -- the average loss for $P_\perp$ = 3 GeV is 3% for the counter system and 20% for the magnet system (the loss goes roughly at $1/P_\perp$). However, again by increasing the size of the chamber to cover the return legs of the magnet, one can make the acceptance of the magnet system as large as that of the counters.

E. Mass Resolution

If one assumes the "parent" of a pair of particles is produced with no horizontal component of transverse momentum, then simply measuring the angle of the second muon tells one its momentum. This is because knowing the transverse momentum of one muon and assuming momentum balance for the air gives the $P_\perp$ for the second muon, which combined with the angle gives the momentum. If θ_1 and θ_2 are the respective angles of the two muons to the beam direction, the mass resolution under the above assumptions is given by

$$\frac{dm}{m} = \frac{d\theta_2}{2\theta_2} \left[\frac{\sqrt{\theta_2/\theta_1} - \sqrt{\theta_1/\theta_2}}{\sqrt{\theta_2/\theta_1} + \sqrt{\theta_1/\theta_2}} \right]$$

Table III presents $\frac{dm}{m}$ as a function of θ_2 for θ_1 = 100 mr, and assuming the precision spectrometer has perfect resolution. One sees that with the above assumptions the mass resolution is staggeringly good.

However, it is reasonable to assume that the parent particle is produced with a $< P_\perp > \simeq$ 500 MeV. In that case, the mass resolution would be $\Delta m/m \simeq \frac{.5}{2P_\perp}$ for the $P_\perp$ set in the precision spectrometer, giving $\frac{\Delta m}{m} \simeq$ 17% at $P_\perp$ = 1.5, $\frac{\Delta m}{m} \simeq$ 8.3% at $P_\perp$ = 3, and $\frac{\Delta m}{m} \simeq$ 5.5% at $P_\perp$ = 4.5 GeV. This is still remarkably good, although it does depend on the(reasonable)assumption about the production of the parent particle.

With the solid steel magnets in place, one can measure all of the variables necessary to calculate the invariant mass of the pair, <u>independent of any assumptions.</u> The mass resolution is dominated both by the error on measuring the momentum due to scattering in the steel of the muon arm magnet, and by the uncertainty in the opening angle due to multiple scattering in the steel shield. The first term depends only on the length and field in the iron magnet; the second term is a weak function of angle. The mass resolution is $\frac{\Delta m}{m} < \pm$ 9% for all angles covered by our detector.

We should note the important point that the magnet system trivially gives a measurement of the sign of the second muon. This measurement could be made over the full aperature of the magnets by using the return legs as well.

V Details of the Apparatus

The details of most of the apparatus are conventional and self-explanatory. Some details, however, deserve comment.

A. The Steel Shield

The total amount of steel required for the shield is $\simeq$ 210 tons. This can be low quality distressed steel. We note that this is an order of magnitude less than recently added to Proton East for muon shielding.

B. Magnet Design

We have not yet prepared a detailed design of the solid steel magnets. However, a sketch showing the general design is given in Fig. 7. The return legs would generally be a little larger in area than the center: one would run at currents such that the center was driven into saturation. The total amount of steel per magnet is $\sim$ 60 tons.

C. Proportional Chambers

The proportional chambers would have 2mm wire spacing, with wires running only in the horizontal plane. Chambers up to 1.5 m wide have been successfully built and tested at the University of Chicago, and we anticipate no problems with the construction. The total number of wires in the system is on the order of 4000.

REFERENCES

1. J. H. Christenson et al., Phys. Rev. D8, 2016 (1973).
2. S. D. Drell and T. M. Yan, Phys. Rev. Letters 24, 181 (1970).
3. G. R. Farrar, CALT-68-422 to be published.
4. B. Richter, talks presented to the 1973 Irvine Conference on Lepton-induced reactions, etc.
5. W. Chen, invited talk to the Chicago APS Meeting, January 1974.
6. For example, see T. Goldman and P. Vinciarelli, SLAC-PUB-1414 (to be published in Phys. Rev. Letters).

FIGURE CAPTIONS

Figure 1. Plan view of the precision spectrometer and the muon arm.

Figure 2. The layout of the muon arm.

Figure 3. The area of the Peyrou plot covered by the muon arm.

Figure 4. The angular distribution $\frac{d\sigma}{d\theta_{lab}}$ for the second muon, as calculated from a parton model by G. Farrar.[3]

Figure 5. The fraction of "other" muons accepted by the muon arm as a function of $P_\perp$, which is the transverse momentum of the muon measured in the precision spectrometer. The muon pairs are assumed to be generated with the angular distribution shown in Figure 4.

Figure 6. Event rates vs $P_\perp$ from parton model predictions[3], assuming 10^{10} π^-/pulse at 200 GeV.

Figure 7 The iron magnet.

TABLE I

Accidental Rates in Counter Bank - Assume 10^{10} Incident Pions/pulse

Counter Bank	$\theta_{Central}$	muons/ster - incident pion $\pi^+ + \pi^-$	K^+	$\Delta\Omega$ lab	$\frac{1}{\sin^2\theta_{cm}}$	μ's/Pulse
1	150 mr	2.0×10^{-5}	1.9×10^{-5}	1.5×10^{-2}	1.21	7.1×10^{3}
2	130 mr	2.2×10^{-5}	2.0×10^{-5}	7.1×10^{-3}	1.07	3.3×10^{3}
3	100 Mr	2.6×15^{-5}	2.5×10^{-5}	3.6×10^{-3}	1.00	1.8×10^{3}
4	70 mr	4.2×10^{-5}	3.9×10^{-5}	1.6×10^{-3}	1.11	1.4×10^{3}
5	50 mr	5.8×10^{-5}	5.2×10^{-5}	8.8×10^{-4}	1.49	1.4×10^{3}
					TOTAL	1.5×10^{4} μ's/pulse

TABLE II

Multiple Scattering in Muon Shield

θ_{lab}	$\langle\theta\rangle_{ms}$	$\langle y\rangle_{ms}$	% lost in hodoscope	% lost in magnet system
.160	.028	5.0"	0%	9%
.140	.026	5.4"	0%	11%
.120	.024	5.8"	0%	14%
.100	.022	6.3"	1%	18%
.080	.020	7.1"	2%	23%
.060	.017	8.2"	4%	30%
.040	.014	10"	9%	39%

TABLE III

Mass Resolution Assuming No Horizontal Transverse Momentum of the Parent

θ_2	$d\theta_{2ms}$	R*	$\frac{dm}{m}$
.160	.028	.23	.02
.140	.026	.17	.015
.120	.024	.09	.009
.100	.022	0	0
.080	.020	.022	.027
.060	.017	.49	.068
.040	.014	.72	.13

$$*R = \left[\frac{\sqrt{\theta_2/\theta_1} - \sqrt{\theta_1/\theta_2}}{\sqrt{\theta_2/\theta_1} + \sqrt{\theta_1/\theta_2}} \right]$$

PION BEAM SPECTROMETER

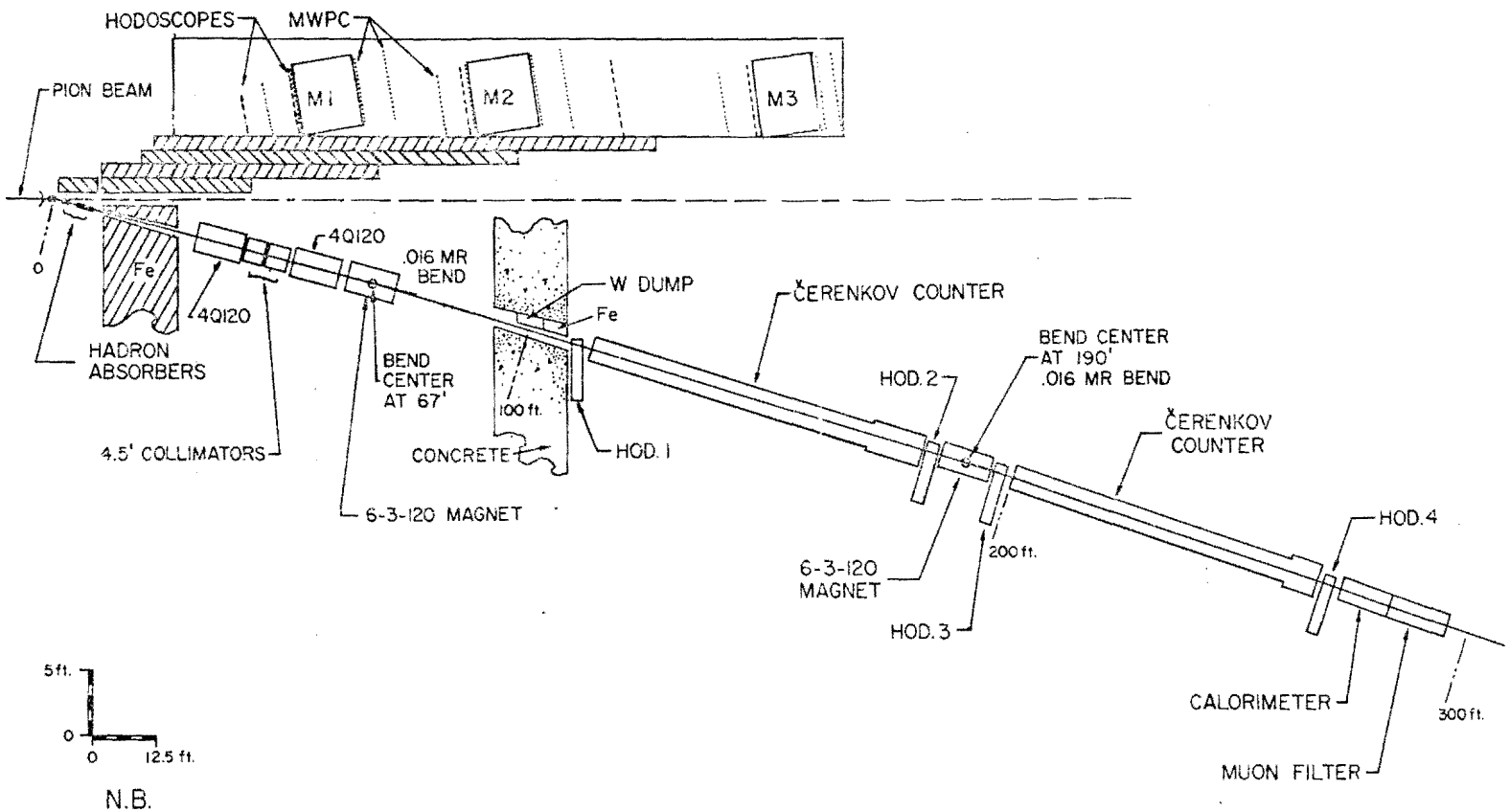

FIGURE 1

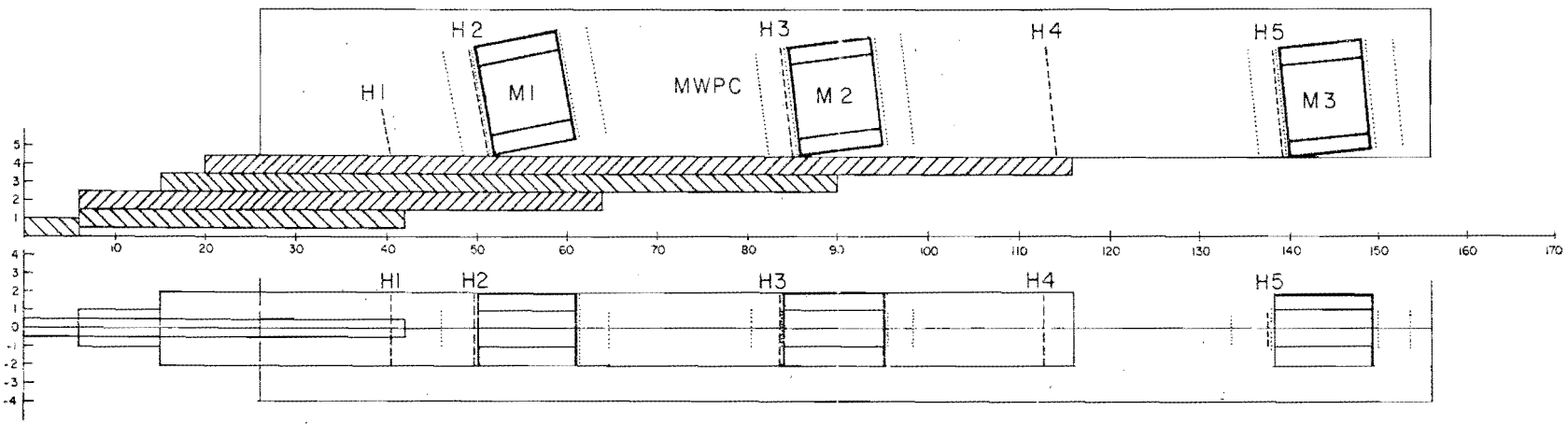

FIGURE 2

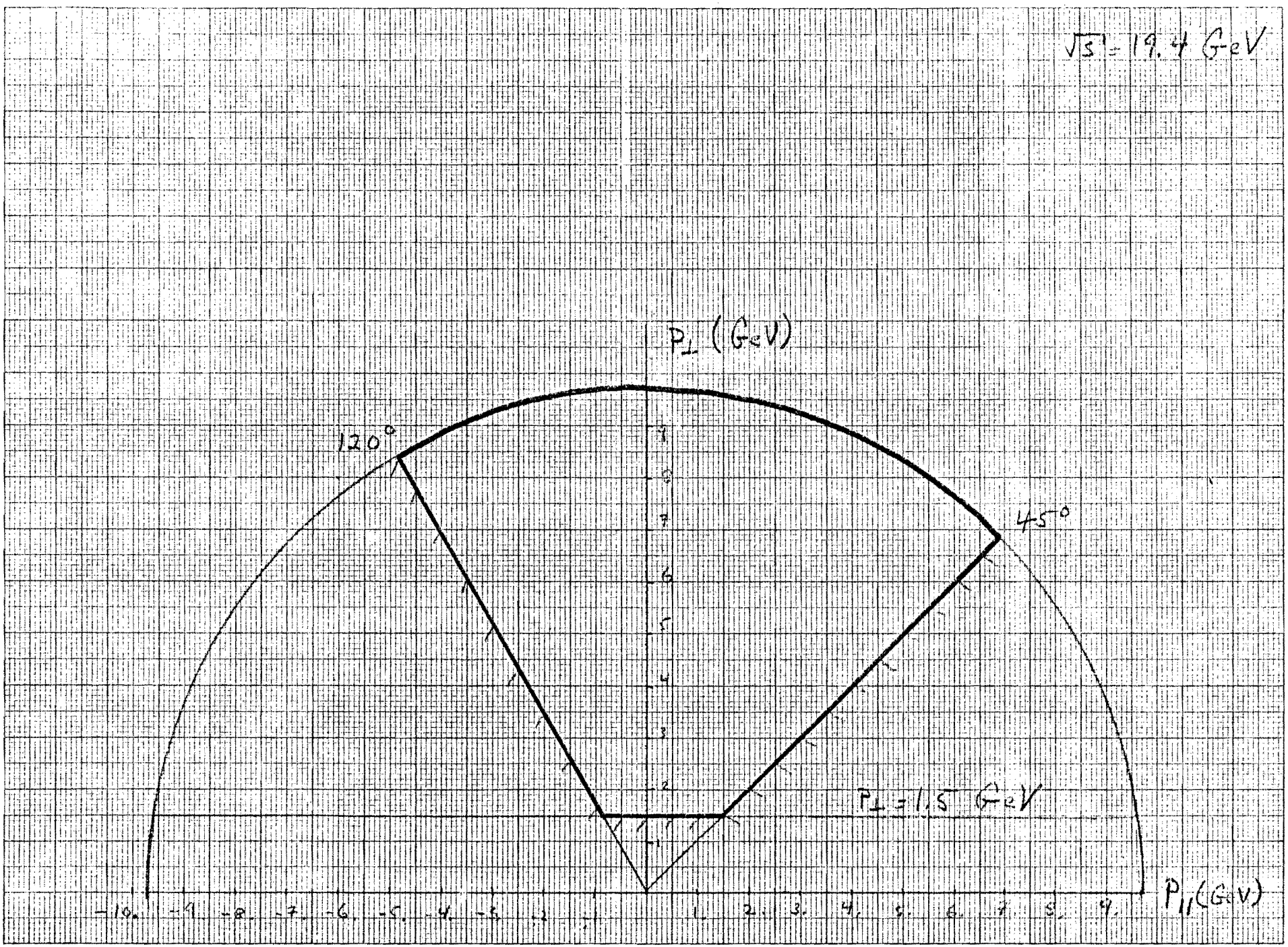

Fig. 3

K+E 10 X 10 TO THE CENTIMETER 18 X 25 CM.
KEUFFEL & ESSER CO. MADE IN U.S.A.
46 1510

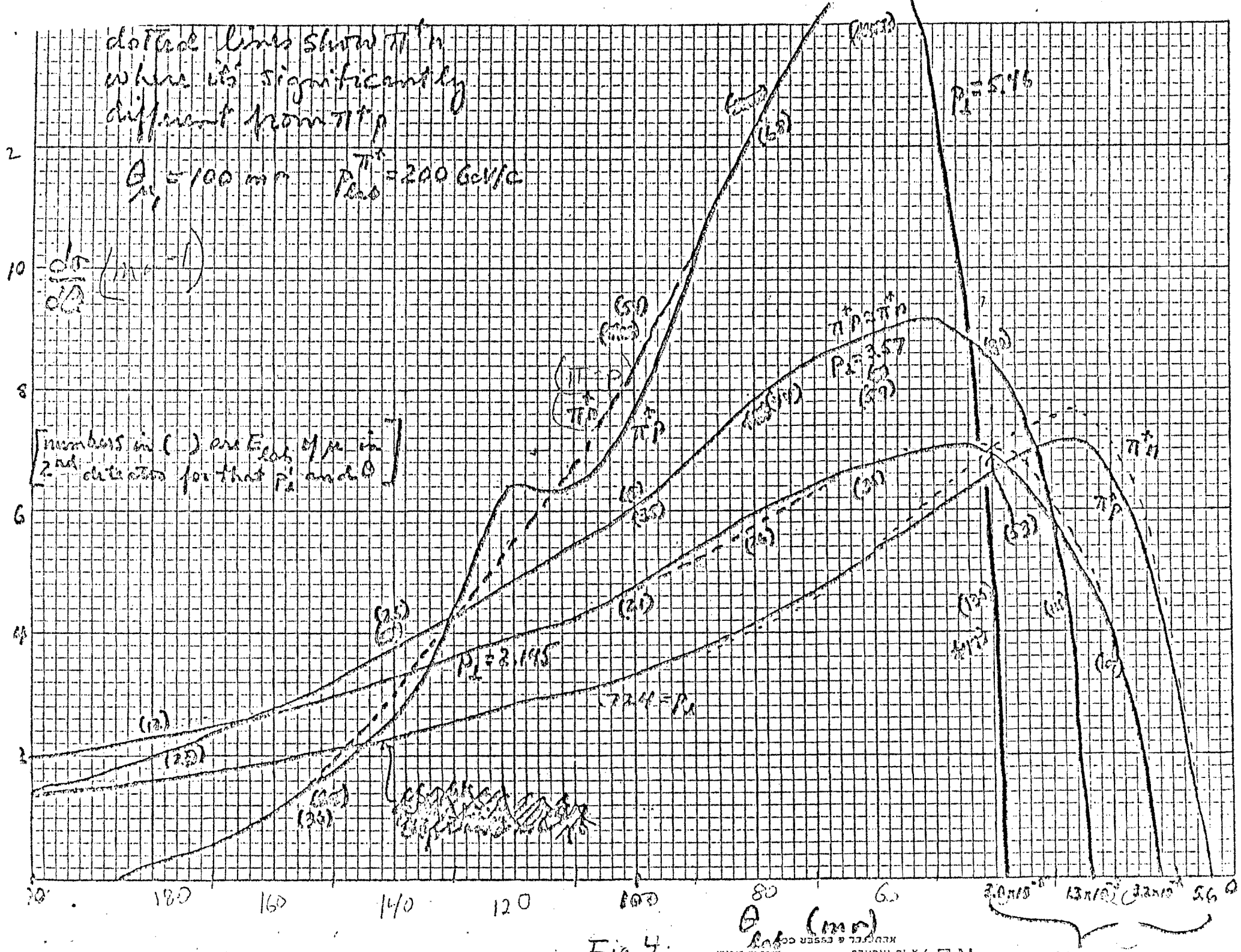
dotted lines show π⁺n
where it's significantly
different from π⁺p
θ_μ1 = 100 mr P_lab^π⁺ = 200 GeV/c
dσ/dθ (mr⁻¹)
[numbers in ( ) are E_lab of μ in 2nd detector for that p⊥ and θ]
π⁺p = π⁺n
P⊥ = 3.57
P⊥ = 5.46
P⊥ = 2.145
.724 = P⊥
π⁺n
π⁺p
θ_lab (mr)
180
160
140
120
100
80
60
5.6
2
10
8
6
4
2

Fig 4.

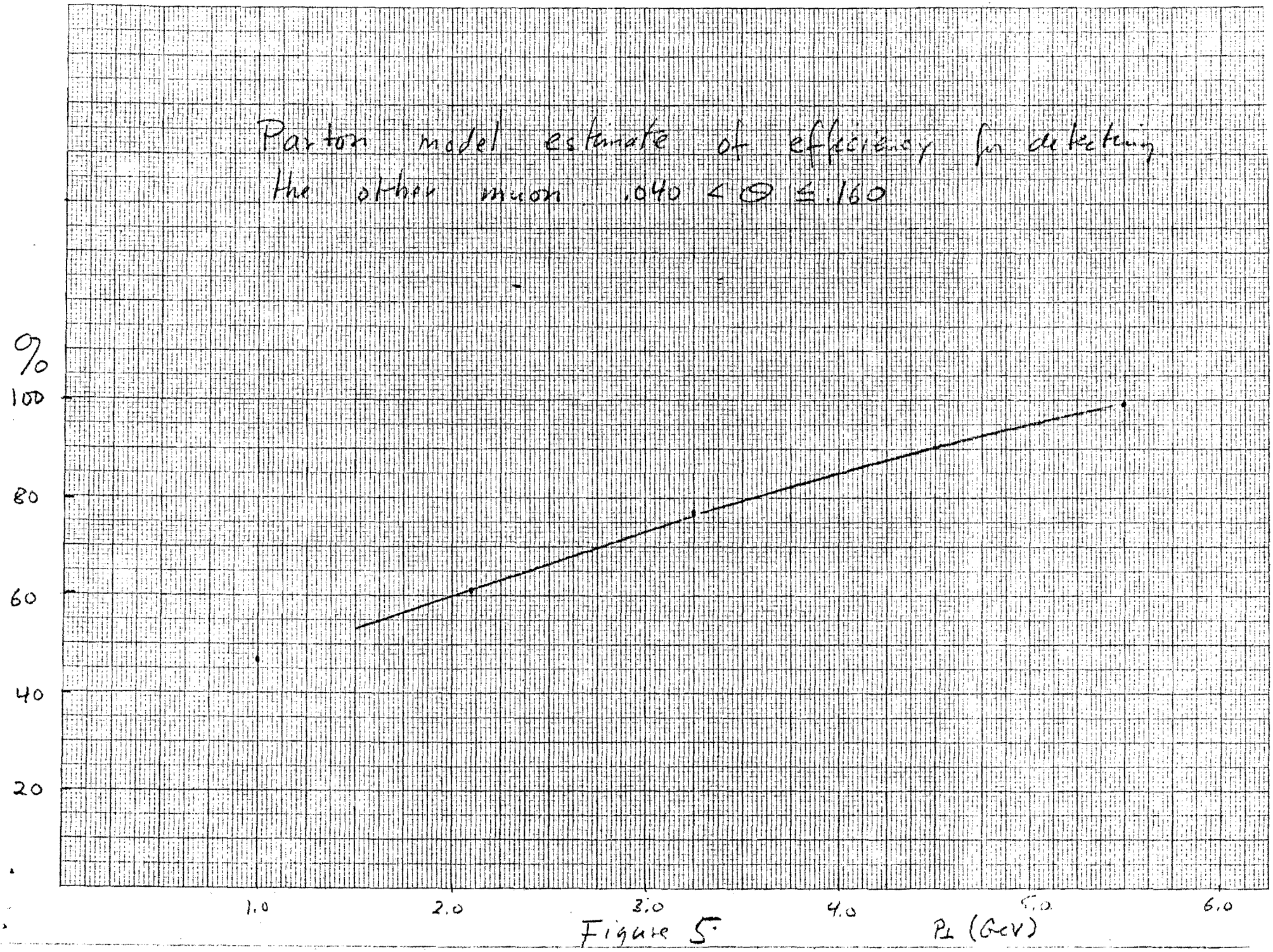
Parton model estimate of efficiency for detecting the other muon .040 < Θ ≤ .160
%
100
80
60
40
20
1.0
2.0
3.0
4.0
5.0
6.0
$P_\perp$ (GeV)

Figure 5

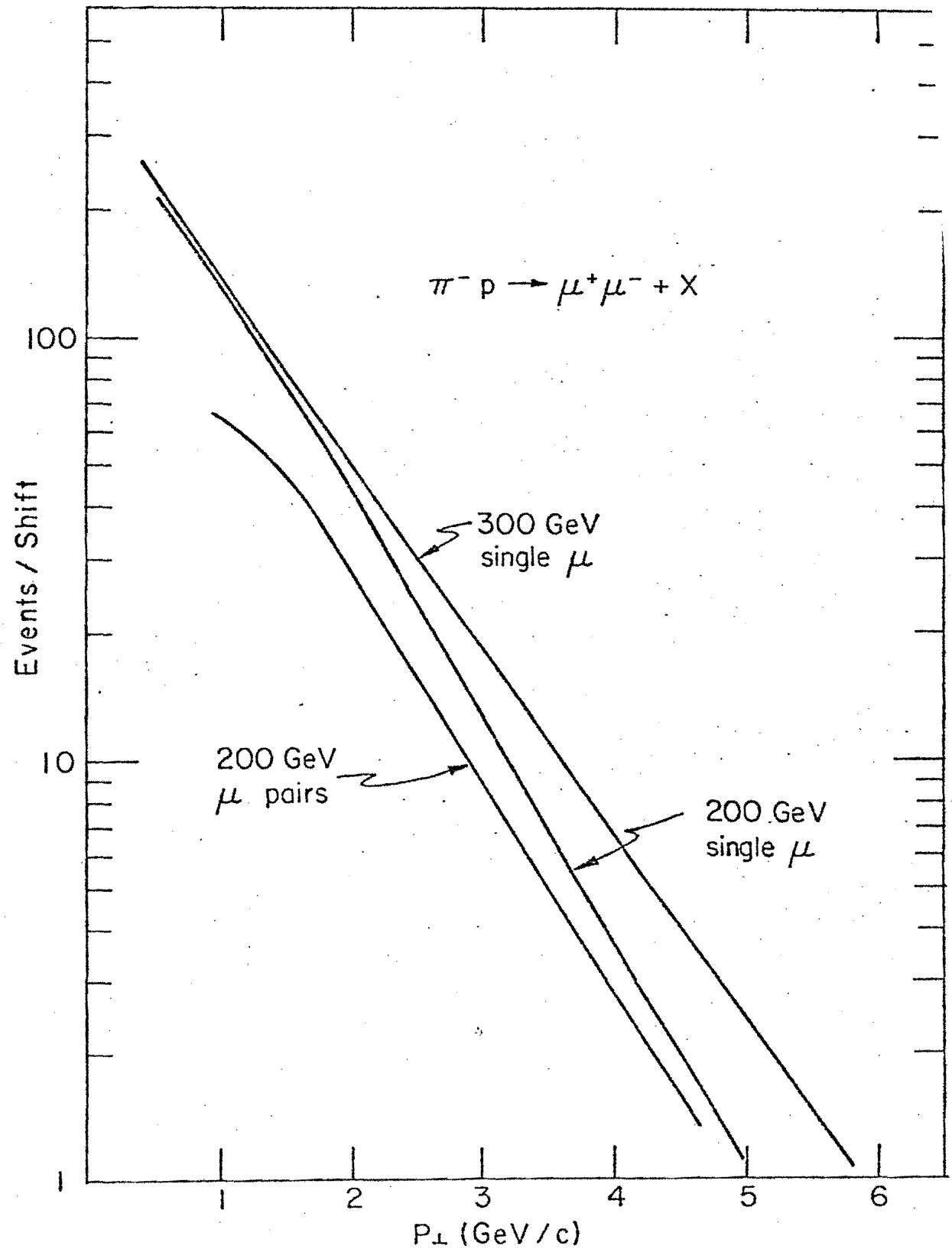
$\pi^- p \rightarrow \mu^+\mu^- + X$
100
10
1
Events / Shift
300 GeV
single μ
200 GeV
μ pairs
200 GeV
single μ
1
2
3
4
5
6
$P_\perp$ (GeV / c)

Figure ~~3~~ 6

46 1510

K+E 10 X 10 TO THE CENTIMETER 18 X 25 CM.
KEUFFEL & ESSER CO. MADE IN U.S.A.

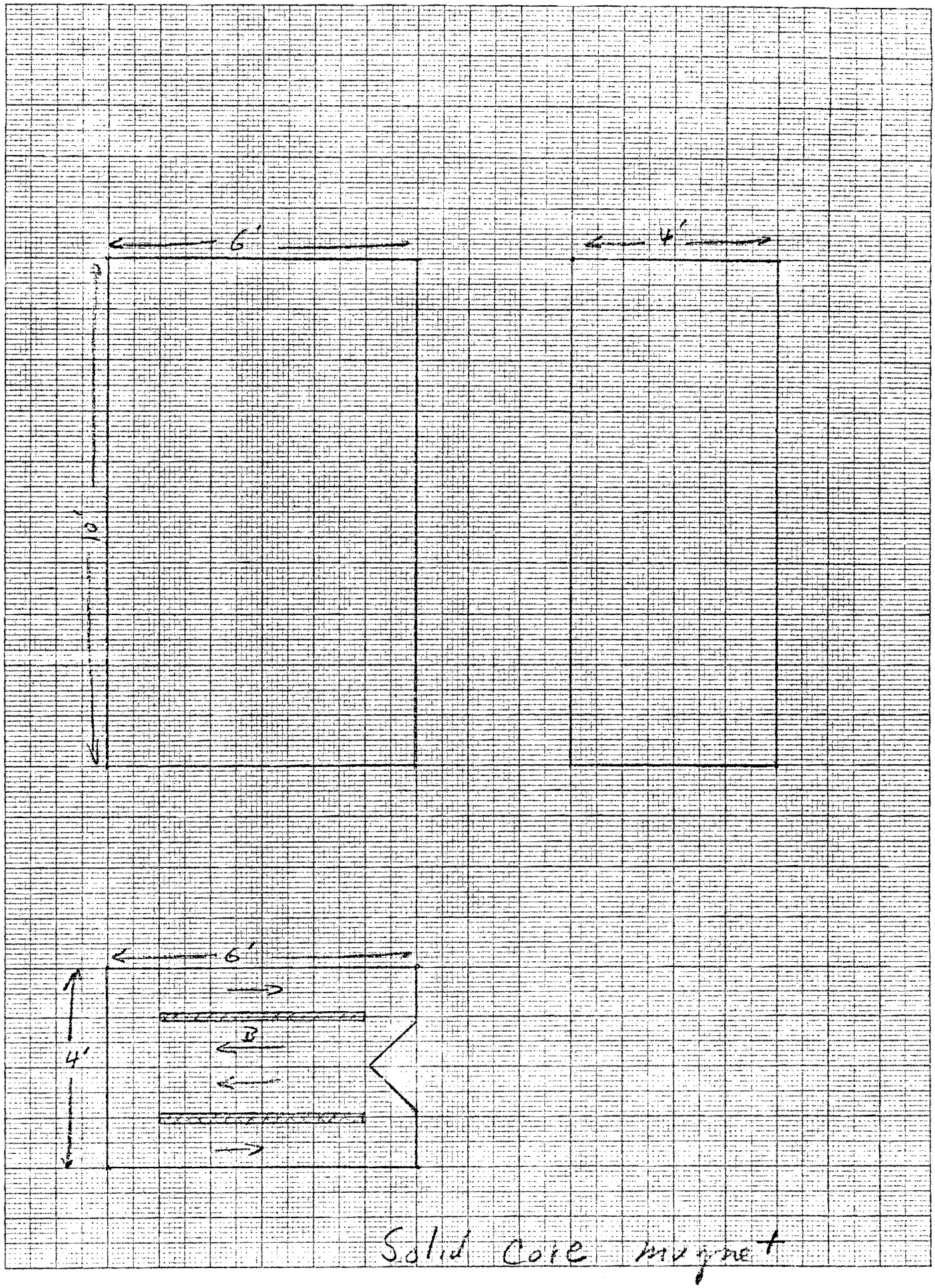

Solid Core magnet

Fig 7